



# EDGEWOOD

## CHEMICAL BIOLOGICAL CENTER

U.S. ARMY RESEARCH, DEVELOPMENT AND ENGINEERING COMMAND

ECBC-TR-821

### INVESTIGATION OF MOLECULE-SURFACE INTERACTIONS WITH OVERTONE ABSORPTION SPECTROSCOPY AND COMPUTATIONAL METHODS

Jerry Cabalo

RESEARCH AND TECHNOLOGY DIRECTORATE

November 2010

Approved for public release;  
distribution is unlimited.

# 20101208346



ABERDEEN PROVING GROUND, MD 21010-5424

#### Disclaimer

The findings in this report are not to be construed as an official Department of the Army position unless so designated by other authorizing documents.



Blank

## PREFACE

The work described in this report was authorized under Job Order No. 0EA171. The work was started in January 2009 and completed in January 2010.

The use of either trade or manufacturers' names in this report does not constitute an official endorsement of any commercial products. This report may not be cited for purposes of advertisement.

This report has been approved for public release. Registered users should request additional copies from the Defense Technical Information Center; unregistered users should direct such requests to the National Technical Information Service.

## Acknowledgments

The author acknowledges the generous help of Dr. Alan Samuels, Dr. Jason Guicheteau, Ronald Miles (U.S. Army Edgewood Chemical Biological Center) and Dr. Barry Williams (Science Applications International Corporation, Gunpowder, MD).

Blank

## CONTENTS

1.	INTRODUCTION .....	7
1.1	Objective .....	7
1.2	Background .....	7
2.	EXPERIMENT AND SIMULATION.....	9
2.1	Theoretical Considerations .....	9
2.1.1	Computational Approach .....	9
2.1.2	Molecule/Surface Modeling.....	10
2.1.3	Theory of the HCAO Model and Calculation of C-H Overtone Frequencies and Intensities .....	11
2.2	Laboratory Measurements .....	16
3.	RESULTS AND DISCUSSION .....	17
3.1	Selection of High Level Method.....	17
3.2	Comparison of FTIR and Near IR Data to Simulated Spectra.....	18
4.	CONCLUSIONS.....	24
	LITERATURE CITED .....	27



## FIGURES

1.	Cluster models for neat TNT .....	16
2.	Comparison of calculated harmonic IR absorption spectra and a TNT film absorption spectrum measured with FTIR.....	18
3.	Comparison of calculated IR absorption spectra (normalized to maximum intensity) and a solid TNT powdered sample measured with photoacoustic FTIR.....	19
4.	Calculated fundamental and first overtones of the C-H stretching absorptions for TNT using the HCAO model vs. near IR transmission measurement of a TNT film.....	21
5.	Comparison of laser PAS spectrum of TNT compared to HCAO simulated spectra.....	25

## TABLES

1.	Predicted harmonic and anharmonic vibrational frequencies for C-H stretches in isolated and clustered TNT molecules.....	22
2.	Morse parameters for HCAO models of an isolated TNT molecule, a TNT molecule within a single unit cell (eight molecules total), and a TNT molecule within an eight unit cell cluster of TNT molecules (64 molecules total).....	23
3.	Calculated transition dipoles in units of Debye <sup>2</sup> /cm.....	23



# INVESTIGATION OF MOLECULE-SURFACE INTERACTIONS WITH OVERTONE ABSORPTION SPECTROSCOPY AND COMPUTATIONAL METHODS

## 1. INTRODUCTION

### 1.1 Objective

The energetics and dynamics of molecule-surface interactions play an integral part to chemical processes and chemical adsorption. Chemical reactions on the surface of a catalyst are a good example of these interactions.<sup>1</sup> A specific set of applications of molecule-surface interactions that is of interest to the warfighter is in chemical-biological defense. For example, chemical personal protective equipment relies heavily on a material's ability to surface bind harmful compounds. Another type of study of interest to the Army's mission is the interaction of energetic material residues with various environmental surfaces. These interactions can have an impact on detectability of the energetic materials. A number of surface techniques have been applied to this problem, such as diffuse reflectance IR spectroscopy<sup>2</sup> and step scan FTIR spectroscopy.<sup>1,3</sup> These techniques have been effective at identifying decomposition intermediates and products even on the timescale of hundreds of nanoseconds. Although these techniques are proven tools for the study of the chemical dynamics of decomposition, details of the molecule/surface interaction are still unknown. Vibrational overtones are uniquely sensitive to a molecule's local environment, and are potentially an effective tool in examining molecule/surface interactions.<sup>4</sup> It is the objective of this work to determine the most effective and general theoretical model of molecular-surface interactions. This will be done using vibrational overtone spectroscopy in tandem with molecular mechanics and ab initio calculations to investigate molecule-surface binding. Due to the importance of 1,3,5-trinitrotoluene (TNT) as a compound and the catalytic and optical properties of alumina, the systems of neat TNT and TNT on an alumina surface serves as the test cases for this study.

### 1.2 Background

The interaction of a molecule with its local environment is reflected in its vibrational spectrum, so that the vibrational spectrum can be used as an indicator of the local environment. Vibrational overtone spectroscopy is ideal for studying molecule-surface interactions because it involves higher vibrational energy levels. When the vibrational potential energy surface of a molecule is perturbed by the presence of a surface or solvent, the higher energy levels experience a more drastic change than the lower levels. This makes sense in view of the fact that at higher vibrational energy levels, the atomic displacement along the vibrational coordinate is greater, so that the molecule-environment interactions will be greater than at lower vibrational energies. These levels are not typically accessed with fundamental absorptions because almost all molecules are in the ground vibrational state at room temperature, so that optical absorption only promotes molecules to the first vibrationally excited state. This energy is quickly lost to equilibrium with the environment so that multiphoton processes are unlikely. As a result, the higher vibrational states are only accessible by overtone transitions, that is, transitions involving more than one quantum of vibrational energy. Although molecules are

typically modeled as harmonic oscillators, real molecules are anharmonic oscillators where transitions of more than one vibrational quantum are possible.<sup>5</sup> As a result, the anharmonic description of molecular vibrations is necessary for this study.

Most theoretical models use the harmonic description of molecular vibrational because it is computationally easier, and because for studies of fundamental transitions it is normally adequate. However, there are additional differences between the anharmonic and harmonic description of molecular vibrations that show that the harmonic description is not sufficient for this study. In the harmonic description, the potential energy surface goes to infinity at large atomic separation and does not account for the breakage of bonds. The result is that the calculated vibrational frequencies for a harmonic oscillator are integer multiples of the fundamental frequency that go up infinitely. In real anharmonic systems, the separation between energy levels tends to zero as the vibrational energy approaches the dissociation limit. This means that the overtone transition frequency will not be an integer multiple of fundamental transition frequency, and that a perturbation is likely to increase the deviation from the frequency predicted by the harmonic treatment. In other words, the harmonic oscillator description will consistently overestimate molecular fundamental and overtone vibrational frequencies. The anharmonic description is essential for adequate handling overtone vibrations.

There are several available approaches for modeling the interaction of a molecule with a surface; however, only some of these methods permit prediction of overtone frequencies. The simplest is molecular mechanics, which operates on a quasi-classical level.<sup>6-9</sup> The details of the electronic states are neglected and the energy of the system is treated as a sum of interactions through chemical bonds, such as bond stretches and bends, and non-bonding interactions such as electrostatic interactions and van der Waals energy. The overall description of the molecule as a sum of classical interactions is also known as a “force field”. The strength of this approach is that it is not computationally expensive to perform, so that large systems can be modeled. A major assumption of this approach is that the interaction between two atoms in one molecule will be like that in another molecule. This assumption leads to two weaknesses of this approach: (1) empirical data is often necessary to build a complete force field, and (2) accuracy of the results depends on the similarity of the system under study to the systems that provided the empirical data. Predicted properties, such as vibrational spectra, are only accurate if the source of the empirical data is very much alike to the model system. Although typical force fields permit use of the Morse Potential for describing bond stretches and anharmonic vibrations, the accuracy is most likely insufficient to make reliable predictions of overtone frequency shifts that can be used to infer the molecule/environment interaction.

The system can also be handled with *ab initio* quantum mechanical or density functional theory (DFT) methods that do not require any empirical data. For *ab initio* methods, the electronic wavefunction of the system is calculated, and the vibrational potential energy surface is directly calculated from the electronic wavefunction.<sup>7,10</sup> For density functional methods, the square of the wavefunction, that is, the probability density, is calculated and used to get the vibrational potential energy surface. For some quantum mechanical methods such as Hartree Fock (HF), DFT, second and third order Moeller/Plesset (MP2/MP3), it is possible to obtain analytic second derivatives and numerical third derivatives of the vibrational potential energy surface. This allows more accurate anharmonic treatment of the potential energy surface,



and calculation of the overtone frequencies. However, these approaches are computationally expensive, so that there is a strong limitation on the size of the theoretical model that can be handled. Fortunately, a number of theoretical modeling packages include the capability to perform hybrid calculations where part of a system is treated with quantum mechanics and another part is treated with molecular mechanics. Proper application of the hybrid treatment permits accuracy approaching that of a purely quantum mechanical method at a fraction of the computational cost.

The overtone frequency serves as the bridge between the molecule-surface interaction model and experiment.<sup>11</sup> A modeling approach will be considered valid if the predicted overtone frequencies accurately reproduce those measured from experiment. A number of important details in the surface/molecule interaction play a part in the simulation that will impact predicted overtone frequencies. For example, the orientation of the molecule relative to the surface will affect how its force field is perturbed, so that each possible orientation will have its own spectral shift. If no particular orientation is favored, then the observed shift in the overtone spectrum will be a convolution of transition energies of all possible orientations. If a particular orientation is favored, as in a catalytic surface, then the shift in the overtone spectrum will reflect this. Another important detail is the magnitude of the molecule-surface binding energy. The binding energy will govern transport dynamics. The binding energy is easily determined in the model by the difference between the energy of the molecule and the surface separated by infinite distance and the energy of the molecule-surface system at the optimized geometry. It is expected that a stronger binding energy will correspondingly perturb the molecular vibrations and result in more drastic shifts in the overtone absorption frequency relative to the isolated molecule.

## 2. EXPERIMENT AND SIMULATION

### 2.1 Theoretical Considerations

#### 2.1.1 Computational Approach

Neat TNT and TNT molecules on an alumina surface are modeled utilizing Gaussian 2003 version B.04 on a Sunstation V, as well as a LAN Parallel cluster utilizing 48 Intel processors, and Gaussian 2009, version A.02. The Sunstation system has 32 Gbytes of RAM memory and eight processors; however, this implementation of Gaussian 2003 does not include the LAN parallel processing code. Each node in the Gaussian 2009 cluster has eight processors and eight Gbytes of RAM. To calculate the overtone absorption frequencies and intensities of TNT interacting with a surface, anharmonic frequency analysis and the Harmonically Coupled Anharmonic Oscillator (HCAO) model are applied. In the HCAO model, each C-H unit within the molecule is treated as a diatomic Morse oscillator that is harmonically coupled to the other C-H units.

The first task is to determine an appropriate level of theory for performing anharmonic frequency and HCAO analysis on the TNT molecule. The criteria for selection are minimal computational expense and accuracy. Accuracy is determined by comparison of the calculated molecular dimensions and fundamental vibrational frequencies to published X-ray data as well as spectroscopic data. Anharmonic frequency calculations are run using Hartree/Fock (HF), second order Moeller/Plesset (MP2), and density functional theory (DFT), methods that have available analytic second derivatives of the potential energy surface. Basis sets up to 6-311+G(d,p) are evaluated. More complex basis sets that have more diffuse functions are not attempted for anharmonic frequency calculations due to computational limitations. Attention is limited to the TNT C-H stretches because they occur at higher frequencies and the resulting overtone absorptions are accessible from wavelengths produced by the optical parametric oscillator (OPO) laser system. For HCAO analysis, DFT with the B3LYP functional is used as a starting point based on the inaccuracy of frequency calculations with HF and the computational cost of utilizing higher levels of theory such as MP2.

The second task is the calculation of absorption frequencies as a function of local environment. Several systems are investigated with the standard frequency analysis within the Gaussian code to calculate the optimal geometry followed by the normal frequencies. Normal mode analysis is then followed by determination of anharmonic corrections. For Gaussian, the second order force constants are determined analytically to give the cubic force constants that are used to determine the anharmonic corrections. Within Gaussian 2003, specifying anharmonic analysis limits the size of the system that can be studied because it attempts to perform the analysis for every mode. Gaussian 2009 permits the user to limit the scope of the anharmonic analysis. Thus, results are obtained from some hybrid quantum mechanical/molecular mechanical models. Several systems are studied with the method, including single molecules, and clusters, where a single TNT molecule is treated with quantum mechanics, and the rest of the cluster is treated with the Universal Force Field (UFF), allowing van der Waals and electrostatic interactions to perturb the quantum mechanical portion of the model. The electrostatic interactions are treated with  $(1/R)$  dependence, and the van der Waals interactions are treated with a "soft" cutoff.

#### 2.1.2 Molecule/Surface Modeling

Several different approaches are evaluated for modeling a surface, such as modeling with periodic boundary conditions (PBC), and hybrid molecular mechanics/quantum mechanics methods. A calculation using the PBC utility is attempted to determine the overtone absorptions in solid neat TNT. X-ray crystallographic measurements of the neat TNT crystal show an eight member unit cell and the spacing between the individual molecules.<sup>12</sup> The published geometry is used as a starting point for the calculation with HF and the STO-3G basis set, which is the lowest level method that can be invoked by the PBC convention. Although half of the Sunstation's resources are used for this calculation (four processors and 16 Gbytes of RAM memory), the calculation is terminated after 20 days without completing the geometry optimization. This approach is not feasible with the computational resources at hand.



The next attempt at modeling a cluster of TNT molecules uses the AM1 Hamiltonian, which is a semi-empirical method. The semi-empirical methods are much less computationally expensive than ab initio methods, and complete on a Windows desktop machine for clusters with three and eight members. The results of the geometric optimization did not compare well with published X-Ray data, and the difference between the resulting structure and the published TNT crystal structural data suggests that a very large cluster is necessary to replicate the published experimental data. The next approach is to speed up the PBC calculation by providing a unit cell optimized with a semi-empirical method. This approach is not workable because the results show significant deviation from the X-ray data.

Calculation using the hybrid quantum mechanics/molecular mechanics (QM:MM) utility of Gaussian is also attempted using combinations of HF:UFF and B3LYP:UFF. To avoid application of the anharmonic analysis to atoms within the model of the surface, Gaussian 2009 is used. Within the newer version of the code, the whole system geometry is optimized with UFF, and then all atoms except the TNT molecule are excluded from further, higher level geometry optimization using HF or B3LYP. The TNT molecule alone undergoes frequency analysis; whereas, the adjacent surface model serves as a perturbation.

### 2.1.3 Theory of the HCAO Model and Calculation of C-H Overtone Frequencies and Intensities

We also use the Harmonically Coupled Anharmonic Oscillator (HCAO) model to simulate overtone transitions from the target molecule, 1,3,5-trinitro-toluene (TNT) interacting with a surface. The HCAO model allows calculation of absorption frequencies and intensities of the overtone transitions, and has been successful in the literature at describing the absorptions of several molecules, including chemical agents.<sup>13-22</sup>

A key assumption of the HCAO model is that for overtones, especially the  $\Delta v > 2$ , the X-H bond stretching coordinates become almost completely independent of the other internal coordinates of the molecule, e.g., bends, torsions, etc. For the purely local mode model, coupling between other internal motion coordinates is completely neglected; whereas, HCAO allows for coupling between X-H oscillators within the molecule, given that they have similar fundamental frequencies. For TNT, there are five C-H oscillators: three oscillators on the methyl group, and two oscillators that are part of the aromatic ring. The three methyl oscillators are treated as kinetically and potentially coupled, and the two aryl oscillators are treated as potentially coupled with the kinetic energy coupling neglected due to the physical separation of the oscillators.

Within the local mode model, the C-H oscillators within TNT are treated as diatomic anharmonic oscillators. The Morse Potential approximates the potential energy surface of a diatomic molecule quite well, even taking into account the dissociation limit, where the Harmonic Oscillator model does not. The potential energy  $V$  as a function of the displacement coordinate  $q$  around the equilibrium bond length, is

$$V(q) = D_e (1 - \exp(-\beta q))^2 \quad (1)$$

where  $q=r-r_0$ , the bond length  $r$  minus the equilibrium bond length  $r_0$ ,  $D_e$  is the dissociation limit measured from the bottom of the potential energy surface, and  $\beta = \sqrt{\frac{8\pi^2 c \mu \omega_e x_e}{h}}$  where  $c$  is the speed of light,  $\mu$  is the reduced mass,  $\omega_e x_e$  is the anharmonicity constant, and  $h$  is Planck's constant,  $6.626 \times 10^{-34}$  J s. Conveniently, there exist analytic solutions to the nuclear Schroedinger for the Morse oscillator. The Hamiltonian of the resulting system for the pure local mode model can be expressed as<sup>23</sup>,

$$\frac{\hat{H}|\nu\rangle - \hat{H}|0\rangle}{hc} = \nu\omega_e|\nu\rangle - \omega_e x_e(\nu^2 + \nu)|\nu\rangle \quad (2)$$

where  $|\nu\rangle$  denote the Morse Oscillator wave functions. Insertion of the appropriate vibrational quantum numbers and Morse Oscillator parameters give the transition frequencies in  $\text{cm}^{-1}$ . For the coupled oscillators in the TNT molecule, the Hamiltonian is written with additional coupling terms, and the nuclear wavefunction for the coupled oscillators are written as products of the individual wave functions along each stretching coordinate. The coupling correction is considered as pairwise interactions between the absorbing C-H oscillator and the rest of the oscillators in the methyl group. The result is Equation 3 for the coupled methyl C-H stretches,

$$\begin{aligned} \frac{\hat{H}|\nu\rangle_i|0\rangle_j|0\rangle_k - \hat{H}|\nu\rangle_i|0\rangle_j|0\rangle_k}{hc} &= \nu\omega_{e(i)}|\nu\rangle_i|0\rangle_j|0\rangle_k - \omega_e x_{e(i)}(\nu^2 + \nu)|\nu\rangle_i|0\rangle_j|0\rangle_k - \dots \\ &\dots - \sum_{i \neq j} \phi'_{ij} (a_i^- a_j^+ + a_j^- a_i^+) |\nu\rangle_i|0\rangle_j|0\rangle_k - \dots \\ &\dots - \sum_{i \neq j} \phi'_{ik} (a_i^- a_k^+ + a_k^- a_i^+) |\nu\rangle_i|0\rangle_j|0\rangle_k \end{aligned} \quad (3)$$

where  $\nu$  is the vibrational quantum number, and  $\omega_{e(i)}$  denotes the Morse oscillator harmonic frequency of the  $i^{\text{th}}$  oscillator, the optical radiation absorbing oscillator,  $\phi_{ij}'$  is the oscillator coupling parameter between the  $i^{\text{th}}$  and  $j^{\text{th}}$  coupled oscillators, and  $a^-$  and  $a^+$  are the harmonic oscillator raising and lower operators, where it is assumed they act on the Morse oscillator wave functions in the same way as the Harmonic wave functions. The combination of raising and lower operators extracts the energy differences between coupled oscillators. Mathematically, the operators behave as,  $a_i^- |\nu\rangle_i = \sqrt{\nu} |\nu-1\rangle_i$  and  $a_i^+ |\nu\rangle_i = \sqrt{\nu+1} |\nu+1\rangle_i$ . For the aryl C-H stretches, the Hamiltonian is the same, except that the nuclear wave functions are products of only two internal coordinate wave functions, and there is only one coupling correction term. The coupling correction term  $\phi_{ij}'$  can be expressed as,

$$\phi_{ij}' = (\gamma_{ij} - \phi_{ij}) \sqrt{\omega_{e(i)} \omega_{e(j)}} \quad (4)$$

where  $\gamma_{ij}$  is the kinetic energy coupling,  $\phi_{ij}$  is the potential energy coupling, and  $\omega_{e(i)}$  and  $\omega_{e(j)}$  are the Morse frequencies of the  $i^{\text{th}}$  and  $j^{\text{th}}$  oscillator. The coupling constants are related to the Wilson G and F matrix elements by,<sup>19,20,23,24</sup>



$$\gamma_{ij} = -\frac{1}{2} \frac{G_{ij}}{\sqrt{G_{ii}G_{jj}}} \quad (5)$$

$$\phi_{ij} = \frac{1}{2} \frac{F_{ij}}{\sqrt{F_{ii}F_{jj}}} \quad (6)$$

where  $G_{ij}$  and  $F_{ij}$  are the off-diagonal matrix elements. For the coupled methyl C-H oscillators located on the same methyl group,  $\gamma_{ij}$  can be written as, from the tabulated G elements,<sup>25-27</sup>

$$\gamma_{ij} = -\frac{1}{2} \cos(\theta) \left( 1 + \frac{m_C}{m_H} \right)^{-1} \quad (7)$$

where  $\theta$  is the angle between the methyl C-H bonds, and  $m_C$  and  $m_H$  are the carbon and hydrogen atomic masses, respectively. The calculation of the fundamental and overtone vibrational frequencies is straightforward. To simplify the determination of force constants from the computational output, the potential energy surface is treated as a Taylor series expansion up to fourth order:<sup>17</sup>

$$V(q) = \frac{1}{2} \frac{\partial^2 V}{\partial q^2} \bigg|_0 q^2 + \frac{1}{6} \frac{\partial^3 V}{\partial q^3} \bigg|_0 q^3 + \frac{1}{24} \frac{\partial^4 V}{\partial q^4} \bigg|_0 q^4 + C \quad (8)$$

where  $C$  is a constant, and the derivatives are the square, cubic, and quartic force constants, evaluated at the equilibrium position, where the linear derivative is 0. The force constants are related to the Morse parameters  $\omega_e$  and  $\omega_e x_e$  by,

$$\omega_e = \frac{\sqrt{G_{ii} \frac{\partial^2 V}{\partial q^2} \bigg|_0}}{2\pi} \quad (9)$$

$$\omega_e x_e = \frac{hG_{ii}}{72\pi^2 c} \left( \frac{\frac{\partial^3 V}{\partial q^3} \bigg|_0}{\frac{\partial^2 V}{\partial q^2} \bigg|_0} \right)^2 \quad (10)$$

where  $G_{ii}$  is one of the diagonal Wilson G matrix elements. In the case of a bond stretching internal coordinate, the G element is  $G_{ii} = (1/m_X + 1/m_H)$ ,<sup>26,27</sup> where  $m_X$  is the atomic mass of X and  $m_H$  is the atomic mass of Hydrogen in the X-H oscillator. The F and G matrices relate the internal coordinates of the molecule to the normal modes.

To extract force constants from the computational output, the geometry of the target molecule and its environment are energy optimized with Gaussian. Then, the potential energy is calculated for a number of grid points around the equilibrium position. In this study, the bond lengths are varied  $\pm 0.30$  Å in steps of 0.05 Å, for a square grid pattern. The potential energy scans are performed along two stretch coordinates simultaneously to be able to capture any interaction between two coordinates. If two local modes are completely uncoupled, then motion along one coordinate has no effect on the other. For the methyl C-H oscillators, each oscillator is scanned pairwise, so that interaction between all three C-H oscillators is captured. The aryl C-H coordinates and an aryl and methyl C-H coordinates are scanned together to check for coupling. For determination of the cubic and square force constants, the potential energy as a function of motion along one coordinate is fitted to equation (8), and all other coordinates are



held at the equilibrium position. The coefficients of the fit generated by Matlab R2006 are substituted into equations (9) and (10) to yield the Morse oscillator parameters. The F matrix elements are determined in a similar way, except that the potential energy surface is fitted along two stretch coordinates simultaneously. Approximating the coupling between oscillators as harmonic, only linear and square terms are used for the fit, yielding the F matrix elements that are used for calculating the coupling corrections in equations (6) and (4). Sufficient information is then on hand for determining the full HCAO predicted oscillator frequency.

To calculate predicted intensities using the HCAO model, the matrix elements of the electric dipole moment operator  $|\langle \psi_1 | \mu | \psi_0 \rangle|^2$  need to be calculated for each oscillator<sup>18</sup>. Because the dipole moment function  $\mu$  is not known analytically, it is approximated with a Taylor expansion up to the fifth order as follows for the three coupled methyl C-H oscillators (11). In the case of the aryl oscillators, their dipole moment function is treated as an expansion along two stretching coordinates with terms taken up to the fourth order (12):

$$|\mu(q_1, q_2, q_3)| = \sum_{i,j,k=1}^{i+j+k=5} \frac{1}{i!j!k!} \left. \frac{\partial^i \mu}{\partial q^i} \right|_0 \left. \frac{\partial^j \mu}{\partial q^j} \right|_0 \left. \frac{\partial^k \mu}{\partial q^k} \right|_0 (q_1 + r_{0(i)})^i (q_2 + r_{0(j)})^j (q_3 + r_{0(k)})^k \quad (11)$$

$$|\mu(q_1, q_2)| = \sum_{i,j=1}^{i+j=4} \frac{1}{i!j!} \left. \frac{\partial^i \mu}{\partial q^i} \right|_0 \left. \frac{\partial^j \mu}{\partial q^j} \right|_0 (q_1 + r_0)^i (q_2 + r_0)^j \quad (12)$$

It must be pointed out that the higher order terms contribute significantly to the intensity calculation. To obtain the dipole moment derivatives, the dipole moment magnitude is determined on the same grid points as the molecular potential energy in the DFT or ab initio calculations. The derivatives are found in the same way as the force constants, except the dipole moment points are fitted to polynomials as denoted by equations (11) and (12). The resulting dipole moment function is used for numerical integration and determination of the transition electric dipole moment. For the calculation of the transition dipole moment, the Morse Oscillator wave functions are used as a basis set. For the Morse wave functions,<sup>28</sup> the phase factor is neglected, and the wave functions are written as (13),

$$\psi(q)_v = |v\rangle = \sqrt{k\beta} \exp\left(-\frac{k}{2} \exp(-\beta q)\right) k \exp(-\beta q)^{\frac{(k-2v-1)}{2}} L_v(k \exp(-\beta q) - (k - 2v - 1)) \quad (13)$$

where  $k$  is the ratio of  $\omega_e$  to  $\omega_e x_e$ ,  $L_v$  is the Laguerre polynomial of the terms within the parentheses. The harmonic basis wave functions along individual coordinates are written as,

$$\psi(q)_v = |v\rangle = \sqrt{\frac{1}{2^v v!}} \left(\frac{2c\mu\omega_e}{\hbar}\right)^{1/4} \exp\left(-\frac{\pi\mu\omega_e q^2}{\hbar}\right) H_v\left(\sqrt{\frac{2\pi\mu}{\hbar}} q\right) \quad (14)$$

where  $\hbar$  is  $h/2\pi$ .<sup>5</sup> The wavefunction then used for the overtone transitions is formed from a linear combination of the harmonic basis functions. For cases where the  $k$  factor becomes large ( $k>175$ ), that is, the ratio of the harmonic frequency to the anharmonicity constant, the exponential factor in the Morse wavefunction expression becomes too small to represent with double precision floating point numbers. In this case, the linear combinations of the harmonic oscillator wave functions are used in the calculation of intensities.

To determine the relative transition intensities, the transition dipole moment  $|\mu_e|^2$  is calculated from the wavefunction expressions for the ground and  $v=2$  excited states and the dipole moment function. For the aryl C-H oscillators, this is equation (15), and (16) for the methyl C-H oscillators,<sup>15,19</sup>

$$|\mu_e| = \langle \nu | \langle 0 |_2 \mu(q_1, q_2) | 0 \rangle_1 | 0 \rangle_2 \quad (15) \quad |\mu_e| = \langle \nu | \langle 0 |_2 \langle 0 |_3 \mu(q_1, q_2, q_3) | 0 \rangle_1 | 0 \rangle_2 | 0 \rangle_3 \quad (16)$$

where the state with the quantum number  $\nu$  indicates the oscillator that absorbs the IR radiation, and the  $\nu=0$  states indicate ground state wave functions. The relative line intensity is then given by equation (17) and is combined with the Lorentzian line shape function to simulate the IR spectra.

$$Intensity \propto \omega_0 |\mu_e|^2 \quad (17)$$

$$I(\omega) = \frac{\omega_0 |\mu_e|^2}{\pi} \frac{\Gamma}{(\omega - \omega_0)^2 + \Gamma^2} \quad (18)$$

where  $\omega_0$  is the transition frequency, and  $\Gamma$  is the full width half max (fwhm) of the absorption feature. Figure 4 shows the simulated spectrum of the C-H stretches in the TNT molecule for a  $80 \text{ cm}^{-1}$  line width, compared with the near IR spectrum. Fundamental and the first overtone transitions are simulated with the HCAO model, for single TNT molecules and clusters of TNT. Figure 1A shows the simplest cluster model simulated for a single eight molecule unit cell, and Figure 1B shows the geometry for an eight unit cell cluster of TNT molecules. The stick models represent the molecules modeled with UFF, and the molecule shown with the ball and stick model represents the molecule that was treated with quantum mechanics. The van der Waals and electrostatic forces are allowed to perturb the quantum mechanical model.

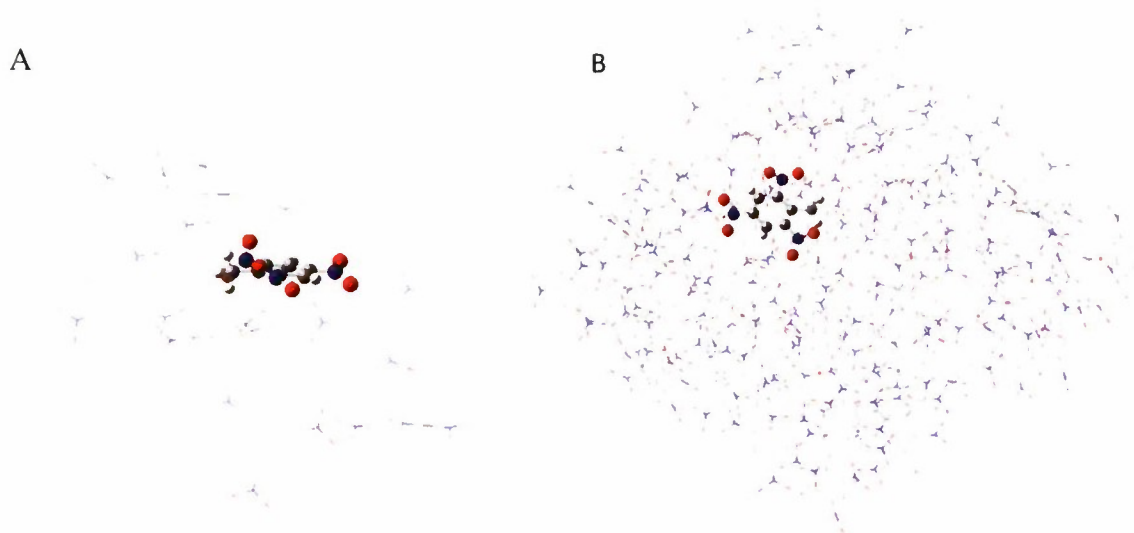


Figure 1. Cluster models for neat TNT. (A) is a single molecule surrounded by a single unit cell, and (B) is surrounded by eight unit cells. The ball and stick model represents the molecule treated with quantum mechanics, and the stick models represent the molecules treated with the classical Universal Force Field.

## 2.2 Laboratory Measurements

Laboratory measurements provide validation of the computational model of the molecule-surface interaction. The validation is provided by agreement of predicted overtone absorption frequencies to experimental measurements. The direct measurement of overtone absorption is accomplished by photoacoustic spectroscopy. When molecules absorb optical energy, they have an increase in internal energy and are out of equilibrium with the environment. The most efficient pathway to equilibrium with the environment is by emitting the excess energy as heat. When the heat is released into fluidic surroundings, such as air or solvent, a pressure wave is created that can be detected with an acoustic transducer.<sup>29</sup> The measurement is directly proportional to the absorbed energy and is completely independent of light scattering from the sample, so that sample morphology has little effect on the measurement of the absorption.<sup>30</sup> When the light source is modulated, the resulting acoustic response will have the same modulation frequency with some delay.

One problem with a photoacoustic approach that must be overcome is that overtone transitions tend to have cross sections one to two orders of magnitude less intense than the fundamental transitions. Comparison between the methods of fundamental and overtone absorption show that this is surmountable. Although measurement of fundamental transitions occur in the mid to far IR portions of the spectrum where laboratory light sources are generally weak, useful measurements are routinely obtained in the laboratory. Overtone transitions tend to occur in the near IR and visible wavelengths, which contain more powerful light sources. Weak signals are overcome with more intense light sources. In systems that are easily saturated with optical energy, the measurement is performed with additional sample to provide measurable photoacoustic signal.<sup>31</sup>



The laser photoacoustic spectra of 50 mg of neat TNT are recorded using the MTEC300, a commercial photoacoustic cell. Tunable excitation radiation of about 0.6 mJ/pulse is produced by the idler of a Spectra Physics 10 Hz GCR-250 Nd:YAG pumped OPO laser system (Spectra Physics MOPO 730), and introduced through a window in the cell. The wavelength is scanned from 435 nm ( $5180\text{ cm}^{-1}$ ) to 465 nm ( $6663\text{ cm}^{-1}$ ). Because the excitation source is a pulsed laser, the acoustic signal is also pulsed, although the acoustic signal has a  $\sim 1$  ms width, compared to the 2.5 ns pulse width of the laser. Signal is acquired with a Stanford Research boxcar integrator with its gate width maximized at 3  $\mu\text{s}$ , to maximize signal to noise. The output of the boxcar is digitized with a National Instruments PCI-4472 digitizer, and the data is acquired with Labview 8.1. Because the signal is not modulated, a resonance condition for signal amplification is not required nor is additional digital signal processing.

Sample characterization is accomplished via photoacoustic FTIR measurements with the same cell that is used for the overtone measurements. For reference, neat TNT samples are also measured with a Perkin-Elmer near IR-Vis spectrometer, and with a Nicolet attenuated transmission/reflectance FTIR.

### 3. RESULTS AND DISCUSSION

#### 3.1 Selection of High Level Method

The first task for the computational component is the determination of the appropriate level of theory for treating the TNT molecule and calculating the overtone frequencies. To obtain the overtone frequencies of the TNT molecule, selection of the theoretical approach is reduced to methods that have analytic second derivatives of the energy with respect to nuclear position, which are Hartree-Fock (HF), Density Functional Theory (DFT), and Moeller/Plesset Theory (MP2/MP3). The anharmonic terms for the potential energy surface are calculated by taking the numerical third derivative of the energy with respect to nuclear position along the normal mode coordinate. The STO-3G, 3-21G, 6-31+G(d,p), and 6-311+G(d,p) basis sets were evaluated for geometry optimization and vibrational frequency calculation utilizing HF, MP2, and DFT, where the B3LYP hybrid functional was used for DFT. The results, such as the fundamental vibrational frequencies and optimized geometric structure, were compared to TNT FTIR spectra measured in the laboratory and published X-ray crystallographic data, respectively. The best results are obtained utilizing B3LYP and MP2 methods with the 6-31+G(d,p) basis set, where calculated bond lengths and angles compare well with the published crystal data,<sup>12</sup> and calculated C-H stretching vibrational frequencies compare well with the laboratory FTIR measurements (within  $20\text{ cm}^{-1}$ , Figure 2). The HF level of theory, without scaling factors, produces differences of  $\sim 225\text{ cm}^{-1}$  between the predicted aromatic C-H stretching frequencies, and the highest frequency in the FTIR spectrum (which we assigned to the aromatic C-H stretching frequency). For the first overtone frequencies, the same trend was also followed where the higher levels of theory resulted in lower predicted frequencies (Table 1). A small peak is visible at  $6036\text{ cm}^{-1}$  in Figure 2, which is close to the overtone frequency for the aromatic asymmetric stretch predicted at  $6161\text{ cm}^{-1}$ . Although the B3LYP and MP2 methods proved to have equivalent accuracy in comparison to published data geometric data, the B3LYP method is the preferred method due to lower computational expense.

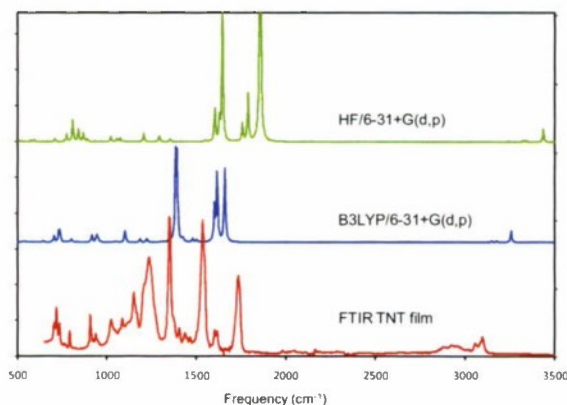


Figure 2. Comparison of calculated harmonic IR absorption spectra and a TNT film absorption spectrum measured with FTIR. The upper trace uses the Hartree-Fock Method, and the middle trace uses Density Functional Theory with the B3LYP functional. Both methods use the 6-31+G(d,p) basis set, which has some diffuse functions.

### 3.2 Comparison of FTIR and Near IR Data to Simulated Spectra

The first phase of experimental data involved collection of TNT spectra with commercial analytical equipment. The mid IR absorption spectrum of TNT was recorded with an Attenuated Transmittance Reflectance (ATR) spectrometer with the data shown in Figure 3. This allowed the spectrum of a thin film of TNT to be recorded. Although several peaks are present in the recorded spectrum that are not visible in the published IR spectrum, which appear to indicate the presence of water and CO<sub>2</sub> in the sample chamber, there is excellent agreement for the C-H stretch frequencies around 3100 cm<sup>-1</sup>. It was also attempted to view the overtone absorptions using a Perkin Elmer near IR spectrometer. The resulting spectrum is shown in Figure 4. Although a peak shows up around ~3100 cm<sup>-1</sup> in this spectrum, corresponding to the aromatic C-H stretches, the signal to noise starts to become rather poor at ~5000 cm<sup>-1</sup> where the light source becomes weak. There appears to be a small peak or divot in the spectrum occurring about where quantum mechanical calculations predict the overtone absorption. This may be an overtone absorption of neat TNT.

Figure 3 compares the results of the standard frequency analysis, with anharmonic corrections, within Gaussian and HCAO spectral simulation compared to the photoacoustic FTIR measurement of the same TNT sample used for laser photoacoustic measurement of the overtone absorption. As shown in the selection of the level of theory and basis set, the HF predicted spectrum differs the most from the FTIR measurement. The aryl hydrogen stretching component of the predicted spectrum from B3LYP is even closer to experiment, yet the contribution from the methyl hydrogens is quite different than the FTIR measurement. Surprisingly, given that the primary assumption of HCAO is that the local mode description is valid only for overtones, the best fit is obtained from the HCAO predicted spectrum of from single TNT molecules. The last simulated spectrum is from a TNT molecule within a 64 member TNT cluster. The model predicts that the contribution from the methyl C-H stretches becomes the dominant spectral feature. This is in complete disagreement with FTIR and near IR measurements. The disagreement between experimental spectra and cluster predicted spectra is even stronger for the overtones.



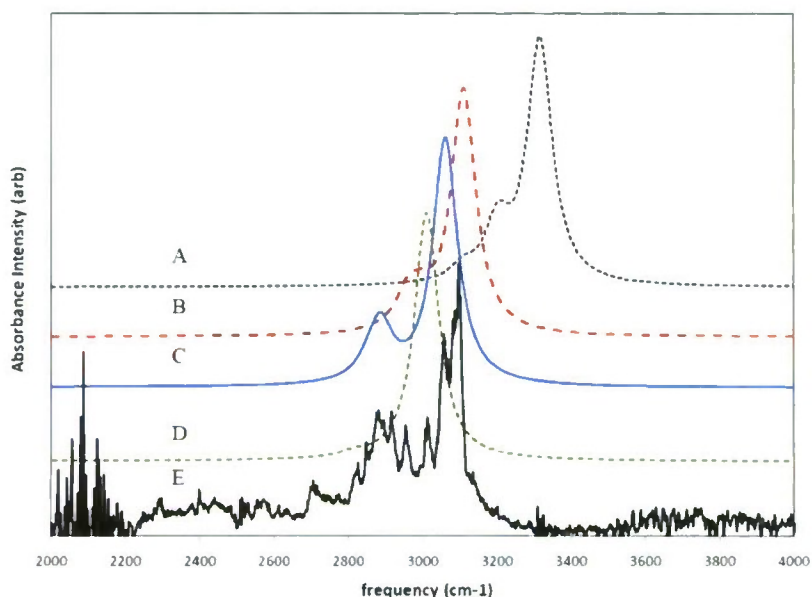


Figure 3: Comparison of calculated IR absorption spectra (normalized to maximum intensity) and a solid TNT powdered sample measured with photoacoustic FTIR. (A) and (B) are spectra predicted by frequency analysis of the normal modes generated with the mass weighted Cartesian coordinates and anharmonic corrections applied at the HF/6-31+G(d,p) and B3LYP/6-31+G(d,p) levels of theory. (C) and (D) are spectra predicted with the HCAO model for a single TNT molecule and a TNT molecule in an 8 unit cell cluster of TNT (64 molecules) at the B3LYP/6-31+G(d,p) level of theory. Trace E is the photoacoustic FTIR measurement.

The experimental overtone spectrum of TNT is compared to several predicted spectra using the HCAO model. The HCAO model as shown in the literature uses the Morse oscillator wave functions as the basis set for the calculation of transition intensity. When potential energy surface (PES) calculations are performed for a TNT molecule within a cluster of TNT molecules, the PES for the C-H stretches becomes more harmonic. Given that the other molecules within the cluster of the model confine the hydrogen along the stretching coordinate, the result is that the depth of the potential well is greatly increased. The increase in well depth makes the PES down at the bottom more harmonic. Because of this, as shown in Table 2, the anharmonicities predicted by the HCAO model become small. The exponential term in equation (13) becomes so small for small anharmonicity values that the values cannot be represented by double precision floating-point numbers. Thus, it is not possible to compensate with normalization of the function, and it became necessary to use linear combinations of harmonic oscillator wave functions. The B spectrum in Figure 5 shows the predicted spectrum from the harmonic oscillator basis set. Instead of an exact match between A and B, the harmonic oscillator wave functions lead to a prediction of greater intensity for the methyl C-H stretches. This is also in disagreement with the experimental measurement, which does not show a strong methyl C-H contribution. Contributions from higher quantum number wave functions may be necessary to bring about agreement from the two methods. Although the overtone spectrum

from a single TNT molecule model with the Morse wavefunction basis set appears to agree with the experimental spectrum quite well, agreement between predicted spectra from TNT within clusters and the experimental data becomes worse. As the cluster becomes bigger, the methyl C-H stretches become increasingly dominant. Correct representation of the wave functions may resolve this issue.

There are additional considerations that may account for increasing discrepancy between predicted spectra from clusters and experimental measurements as shown in Figure 5. The cluster models so far have only examined the spectral contribution from single molecules, instead of an average over an ensemble of molecules. Thus, the predicted spectra may be overly sensitive to the local environment of a single molecule. This is especially true of the predicted intensities, or transition dipoles, as shown in Table 3, where the aryl C-H transitions are predicted to have much less intensity relative to the methyl C-H stretches. The averaging of several predicted molecular spectra may be necessary to adequately predict spectra. An additional consideration is that the van der Waals and electrostatic interaction terms in the UFF force field may cause an overestimation of how much the surrounding molecules in the cluster perturb the molecule under study. The non-bonding interactions between atoms are considered pairwise. As a result, three body effects, such as the screening of one atom by another are not accounted for. It may be necessary to introduce sharper cutoff distances for the non-bonding contributions to the force field, or to increase the size of the quantum mechanical model to include surrounding molecules. The hybrid molecular mechanics/quantum mechanics treatment also uses the qEq algorithm to assign partial charges to the UFF layer in the model. It is known that this algorithm has a margin of error for this, and may be over predicting the effect of charge on the TNT molecule in the quantum layer of the calculation. Expansion of the quantum mechanical layer will allow the partial charges on the surrounding molecules to be determined directly from ab initio methods.



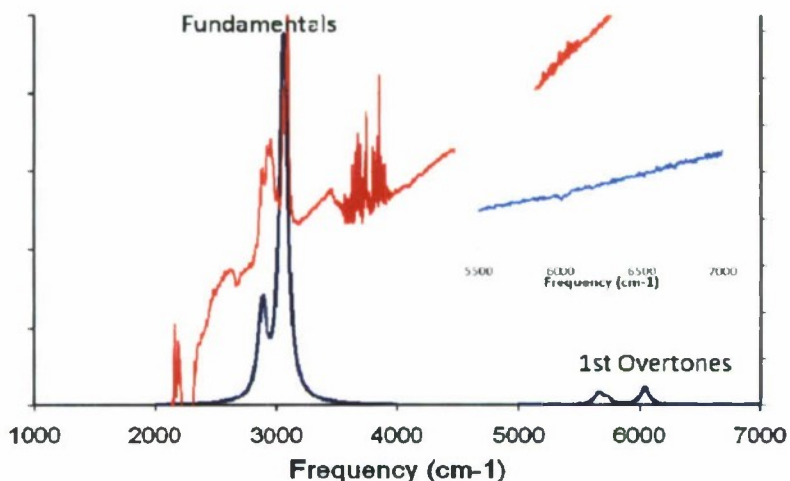


Figure 4: Calculated fundamental and first overtones of the C-H stretching absorptions for TNT using the HCAO model vs. near IR transmission measurement of a TNT film. The inset shows a small feature in the near IR spectrum that appears at  $\sim 6000\text{ cm}^{-1}$ , on a predicted overtone feature. The predicted overtone intensity relative to the fundamental is about 5%.

With respect to the standard anharmonic frequency analysis within the Gaussian code, except for very small clusters, calculations involving standard anharmonic analysis do not successfully complete. Considerable effort was devoted to determining the cause of this failure. Although the geometry optimization of the model system typically completes, problems are encountered during the frequency analysis. These calculations were rerun at the High Performance Computing Center at Aberdeen in an attempt to diagnose the issue, using  $\sim 100$  cores and the LAN parallel version of Gaussian 2009. A similar failure occurred, where the calculation did not complete after several weeks of execution. We suspect that the core issue is the method Gaussian uses to determine the anharmonic corrections to the normal mode frequencies. To determine the anharmonic corrections, Gaussian needs to find the analytic representation of the second order mass weighted force constants in Cartesian coordinates, to find the third order force constants. For models involving large numbers of nonbonding interactions, the necessity of analytic second order force constants may be an impossible constraint. In contrast, within the HCAO model, determination of the third order force constant merely involves fitting a fourth order polynomial to a PES along a single coordinate. As a result, HCAO analysis is performed on systems that could not be viewed with the standard analysis.

Table 1. Predicted harmonic and anharmonic vibrational frequencies for C-H stretches in isolated and clustered TNT molecules. Columns are in order of decreasing frequencies, where columns 1 and 2 involve the aromatic hydrogens, and 3-5 correspond to motions of the methyl hydrogens. HCAO Morse and HCAO Harmonic are HCAO models using either Morse oscillator wave functions or harmonic oscillator wave functions as basis sets. Linear combinations of harmonic oscillators are necessary for the HCAO analysis when the anharmonicity constants become small.

		<i>C-H Stretching Frequency(<math>\text{cm}^{-1}</math>)</i>				
<i>Single Molecule</i>		<i>1</i>	<i>2</i>	<i>3</i>	<i>4</i>	<i>5</i>
<i>HF/6-31+G(d,p) Anharmonic</i>		3321.21	3314.09	3205.23	3202.74	3111.26
	<i>1st Overtone</i>	6580.28	6570.02	6349.26	6349.26	6362.47
<i>B3LYP/6-31+G(d,p) Anharmonic</i>		3114.60	3110.40	3003.40	2963.00	2963.00
	<i>1st Overtone</i>	6172.00	6161.50	5977.10	5960.60	5878.00
<i>B3LYP/6-31+G(d,p) HCAO Morse</i>		3061.50	3061.50	2855.20	2887.20	2887.53
	<i>1st Overtone</i>	6039.39	6039.39	5660.11	5727.34	5728.06
<i>B3LYP/6-31+G(d,p) HCAO harmonic</i>		3061.50	3061.50	2855.20	2887.20	2887.50
	<i>1st Overtone</i>	6039.40	6039.40	5660.10	5727.30	5728.10
<i>Molecular Cluster</i>						
<i>HF/6-31+G(d,p) Anharmonic 1 unit cell</i>		3325.14	3318.83	3312.34	3207.11	3150.32
	<i>1st Overtone</i>	6550.39	6538.50	6530.42	6371.49	6286.35
<i>B3LYP/6-31+G(d,p) 1 unit cell Anharmonic</i>		3124.68	3120.81	3116.98	3014.98	2987.63
	<i>1st Overtone</i>	6138.36	6125.90	6123.00	5959.52	5954.17
<i>B3LYP/6-31+G(d,p) 1 unit cell HCAO</i>		3006.35	3002.73	2901.39	2812.44	2811.47
	<i>1st Overtone</i>	6012.71	6005.45	5842.06	5661.82	5659.94
<i>B3LYP/6-31+G(d,p) 8 unit cell HCAO</i>		3011.00	3011.40	2812.90	2817.90	2801.20
	<i>1st Overtone</i>	6022.00	6021.10	5658.80	5673.20	5636.30

Table 2. Morse parameters for HCAO models of an isolated TNT molecule, a TNT molecule within a single unit cell (eight molecules total), and a TNT molecule within an eight unit cell cluster of TNT molecules (64 molecules total). Note that for the models involving clusters, the anharmonicity constant becomes small. This effect affects the method of calculating the absorption intensities.

<i>Morse Parameters</i>	<i>1</i>	<i>2</i>	<i>3</i>	<i>4</i>	<i>5</i>
<i>B3LYP/6-31+G(d,p) <math>\omega_e</math> (cm<sup>-1</sup>)</i>	3229.20	3229.20	3094.50	3131.10	3131.30
<i>Anharmonicity <math>\omega_e x_e</math> (cm<sup>-1</sup>)</i>	83.73	83.73	87.72	87.45	87.41
<i>B3LYP/6-31+G(d,p) 1 unit cell <math>\omega_e</math> (cm<sup>-1</sup>)</i>	3006.40	3002.80	2971.70	2893.20	2892.10
<i>Anharmonicity <math>\omega_e x_e</math> (cm<sup>-1</sup>)</i>	0.01	0.02	0.87	4.77	4.72
<i>B3LYP/6-31+G(d,p) 8 unit cell <math>\omega_e</math> (cm<sup>-1</sup>)</i>	3010.30	3010.40	2893.80	2896.70	2887.00
<i>Anharmonicity <math>\omega_e x_e</math> (cm<sup>-1</sup>)</i>	0.23	0.09	6.65	4.00	7.54

Table 3. Calculated transition dipoles in units of Debye<sup>2</sup>/cm. The first two rows are for single TNT molecules using the Morse and harmonic wave function basis sets, respectively. Models with a large molecular cluster around the TNT molecule used only harmonic oscillator wave function basis sets to calculate intensity.

	<i>1</i>	<i>2</i>	<i>3</i>	<i>4</i>	<i>5</i>
<i>B3LYP/6-31+G(d,p) HCAO Morse</i>	2.954713	2.954539	0.259592	0.663128	0.664081
<i>1st Overtones</i>	0.143255	0.143281	0.193207	0.046579	0.046634
<i>B3LYP/6-31+G(d,p) HCAO HB</i>	132.7	132.7	34.039	22.293	22.281
<i>1st Overtones</i>	1.6258	1.6257	0.14619	0.14635	0.14622
<i>B3LYP/6-31+G(d,p) 1 cell HCAO</i>	3.501575	3.617291	0.183668	1.719555	3.03683
<i>1st Overtones</i>	0.010915	0.010844	0.15329	0.074628	0.066534
<i>B3LYP/6-31+G(d,p) 8 cell HCAO</i>	7.7497	2.9994	0.50615	0.010906	0.000812
<i>1st Overtones</i>	0.001149	0.000108	1.1818	1.4892	0.07721



#### 4. CONCLUSIONS

Spectroscopic measurements of the fundamental and first overtone C-H stretching are measured with photo acoustic FTIR, photoacoustic laser spectroscopy, transmission FTIR spectroscopy, and near IR transmission spectroscopy. Single TNT molecules as well as several TNT cluster systems are investigated with theoretical chemistry with the objective generating predicted IR spectra from the C-H stretching modes for comparison to experiment. HCAO and standard frequency analysis are applied to models of single TNT molecules, eight molecule clusters of TNT, and 64 molecule clusters of TNT. Only the HCAO analysis successfully predicted overtone spectra for comparison to experimental measurement. The standard anharmonic frequency analysis has been unsuccessful in predicting spectra, most likely due to limitations with the core method of determining the anharmonic corrections themselves. Although HCAO analysis has successfully produced predicted spectra, the spectra for clusters are not yet in good agreement with spectroscopic measurements. The disagreement may arise either from (1) an overestimation of the nonbonding interactions between molecules in the cluster; (2) fact that the spectra are calculated from single molecules rather than an ensemble of molecules; (3) because the boundary between the quantum mechanical and the classical mechanical models has not been well chosen; or (4) because an inadequate basis set of harmonic oscillator wave functions has been used in the intensity calculations.

The issues identified above will be resolved as follows. When using the nonbonding interactions of a force field to perturb the quantum mechanical portion of the model, the contribution from each atom in the molecular mechanics layer is considered pairwise. The effect of this approach is to ignore screening effects from other atoms, and overestimate the total nonbonding interaction. Additional calculations will be run that introduce steeper cutoffs for nonbonding interactions in the force field model. Another possible source of inaccuracy may be poor selection of the boundary between the quantum mechanical layer and the molecular mechanics model. This can be remedied with additional calculations that surround the target molecule with an additional layer of quantum mechanical molecules. We expect more accurate, partial charges on the neighboring molecules. Another consideration is the contribution of multiple molecules to the overtone spectra. As stated previously, the overtone spectrum is sensitive to the local environment, and as a result, each molecule that contributes to the spectrum may have a much different individual spectrum. To address this issue, additional calculations will explore how the spectrum changes if it results from an average over several molecules in the model. Finally, if the above approaches do not resolve discrepancies between predicted overtone spectra from clusters, the effect of the harmonic oscillator basis set in the intensity calculation will be investigated. Higher quantum number wave functions will be included in the linear combination.

The stated objective of this study is to 1) validate computational models by agreement between experimental and predicted overtone spectra, and 2) to apply the model to the test case of TNT on alumina. To obtain these objectives, additional work needs to be done. First, additional overtone spectra of TNT on alumina need to be measured, where the primary spectral contribution is from TNT molecules interacting with the surface. Second, additional modifications to the HCAO model are necessary to produce better agreement between predicted

spectra and experiment. Lastly, once predicted spectra have better agreement with experiment, to use the models to predict interaction properties, such as binding energy.

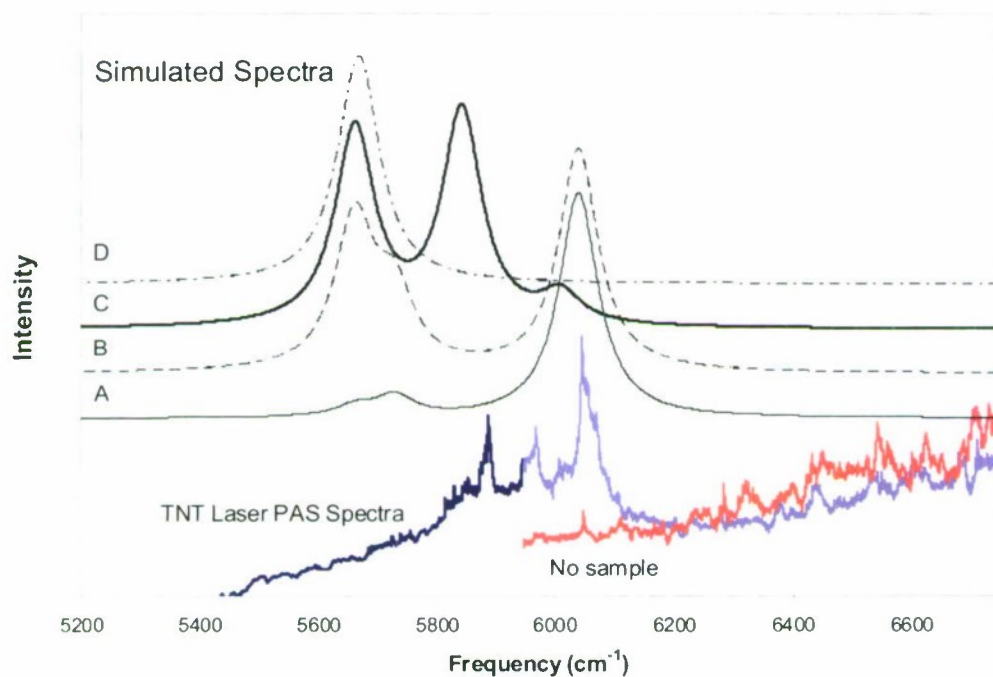


Figure 5. Comparison of laser PAS spectrum of TNT compared to HCAO simulated spectra. Trace (A) is the spectrum obtained from a single TNT molecule and a Morse Oscillator basis set, (B) is the same molecule with a Harmonic oscillator basis set, (C) is a TNT molecule in a 1 unit cell cluster, and (D) is a single molecule within an 8 unit cell cluster, where all predicted spectra have been normalized with respect to the most intense peak.

Blank

## LITERATURE CITED

1. Mendoza-Alvarez, J. G.; Cruz-Orea, A.; Zelaya-Angel, O.; Torres-Delgado, G.; Castanedo-Perez, R.; Hernandez, S. A.; Marquez-Marin, J. Characterization of TiO<sub>2</sub> Thin Films for Photocatalysis Applications Using Photoacoustic Spectroscopy. *Journal de Physique IV* **2004**, *125*, 407-409.
2. Skaare Rygh, L. E.; Gausemel, I.; Ellestad, O. H.; Klæboe, P.; Nielsen, C. J.; Rytter, E. Diffuse Reflectance IR Studies of Bimetallic Fischer-Tropsch Catalysts. *J. Mol. Struct.* **1995**, *349*, 325-328.
3. Zhang, P.; Urban, M. W. Photoacoustic FT-IR Depth Imaging of Polymeric Surfaces: Overcoming IR Diffraction Limits. *Langmuir*, *20* (24), 10691-10699.
4. Pipino, A. C. R.; Hoefnagels, J. P. M.; Watanabe, N. Absolute Surface Coverage Measurement Using a Vibrational Overtone. *J. Chem. Phys.* **2004**, *120* (6), 2879-2888.
5. Atkins, P. W. Physical Chemistry; Fourth ed.; W. H. Freeman and Company: New York, 1990.
6. Morales, C. M.; Thompson, W. H. Mixed Quantum-Classical Molecular Dynamics Analysis of the Molecular-Level Mechanisms of Vibrational Frequency Shifts. *J. Phys. Chem. A* **2007**, *111* (25), 5422-5433.
7. Cramer, C. J. Essentials of Computational Chemistry; Second ed.; John Wiley and Sons: New York, 2004.
8. Rappe, A. K.; Casewit, C. J.; Colwell, K. S.; Goddard, W. A. I.; Skiff, W. M. UFF, a Full Periodic Table Force Field for Molecular Mechanics and Molecular Dynamics Simulations. *J. Am. Chem. Soc.* **1992**, *114* (25), 10024-10035.
9. Mayo, S. L.; Olafson, B. D.; Goddard, W. A. I. DREIDING: A Generic Force Field for Molecular Simulations. *J. Phys. Chem.* **1990**, *94* (26), 8897-8909.
10. Clark, T. A Handbook of Computational Chemistry; John Wiley and Sons: New York, 1985.
11. Howard, D. L.; Jorgensen, P.; Kjaergaard, H. G. Weak Intramolecular Interactions in Ethylene Glycol Identified by Vapor Phase OH-Stretching Overtone Spectroscopy. *J. Am. Chem. Soc.* **2005**, *127* (48), 17096-17103.
12. Carper, W. R.; Davis, L. P.; Extine, M. W. Molecular Structure of 2,4,6-Trinitrotoluene. *J. Phys. Chem.* **1982**, *86* (4), 459-462.



13. Zhu, C.; Kjaergaard, H. G.; Henry, B. R. CH-Stretching Overtone Spectra and Internal Methyl Rotation in 2,6-Difluorotoluene. *J. Chem. Phys.* **1997**, *107* (3), 691-701.
14. Kjaergaard, H. G.; Henry, B. R.; Wei, H.; Lefebvre, S.; Carrington, T. Jr.; Mortensen, O. S.; Sage, M. L. Calculations of Vibrational Fundamental and Overtone Band Intensities of H<sub>2</sub>O. *J. Chem. Phys.* **1994**, *100* (9), 6228-6239.
15. Petryk, M. W. P.; Henry, B. R. CH Stretching Vibrational Overtone Spectra of Tert-Butylbenzene, Tert-Butyl Chloride, and Tert-Butyl Iodide. *J. Phys. Chem.* **2005**, *109* (18), 4081-4091.
16. Kjaergaard, H. G.; Henry, B. R. The Relative Intensity Contributions of Axial and Equatorial CH Bonds in the Local Mode Overtone Spectra of Cyclohexane. *J. Chem. Phys.* **1992**, *96* (7), 4841-4851.
17. Sowa, M. G.; Henry, B. R.; Mizugai, Y. Vibrational Overtone Study of Five-Membered Aromatic Heterocycles: Local Mode Interpretations. *J. Phys. Chem.* **1991**, *95*, 7659-7664.
18. Petryk, M. W. P. Vibrational Overtone Stretching Transitions in Sarin. *Prog. Biomed. Optics and Imaging* **2006**, *7* (43), 637818.1-637818.14.
19. Mortensen, O. S.; Henry, B. R.; Mohammadi, M. A. The Effects of Symmetry within the Local Mode Picture: A Reanalysis of the Overtone Spectra of the Dihalomethanes. *J. Chem. Phys.* **1981**, *75*, 4800-4808.
20. Kjaergaard, H. G.; Proos, R. J.; Turnbull, D. M.; Henry, B. R. CH Stretching Overtone Investigation of Relative CH Bond Lengths in Pyridine. *J. Phys. Chem.* **1996**, *100*, 19273-19279.
21. Kjaergaard, H. G.; Henry, B. R. CH Stretching Overtone Spectra and Intensities of Vapor Phase Naphthalene. *J. Phys. Chem.* **1995**, *99*, 899-904.
22. Henry, B. R.; Tarr, A. W.; Mortensen, O. S.; Murphy, W. F.; Compton, D. A. C. Raman and Infrared Excitation of Local Mode States in Neopentane. *J. Chem. Phys.* **1983**, *79* (6), 2583-2589.
23. Child, M. S.; Lawton, R. T. Local and Normal Vibrational States: A Harmonically Coupled Anharmonic-oscillator Model. *Faraday Discuss. Chem. Soc.* **1981**, *71*, 273-285.
24. Petryk, M. W. P.; Henry, B. R. C-H Stretching Vibrational Overtone Spectra of Tert-Butylbenzene, Tert-Butyl Chloride, and Tert-Butyl Iodide. *J. Phys. Chem.* **2005**, *109*, 4081-4091.

25. Wilson, E. B.; Decius, J. C.; Cross, P. C. *Molecular Vibrations*; McGraw-Hill: New York, 1955.
26. Wilson, E. B. A Method of Obtaining the Expanded Secular Equation for the Vibration Frequencies of a Molecule. *J. Chem. Phys.* **1939**, *7*, 1047-1052.
27. Decius, J. C. A Tabulation of General Formulas for Inverse Kinetic Energy Matrix Elements in Acyclic Molecules. *J. Chem. Phys.* **1948**, *16* (11), 1025-1034.
28. Brabson, G. D. Calculation of Morse Wave Functions with Programmable Desktop Calculators. *J. Chem. Ed.* **1973**, *50* (6), 397.
29. Rosenewaig, A. Photoacoustics and Photoacoustic Spectroscopy. [57], 1-307. 1980. New York: John Wiley and Sons. Chemical Analysis. Elving, P. J., Winefordner, J. D., and Kolthoff, I. M. Ref Type: Serial (Book, Monograph)
30. Natale, M.; Lewis, L. N. Applications of PAS for the Investigation of Overtones and Combinations in the Near IR. *Appl. Spectrosc.* **1982**, *36* (4), 410-413.
31. Hsueh, Y.-M.; Harata, A.; Kitamori, T.; Sawada, T. Photoacoustic Determination of Trace Species Adsorbed on a Single Microparticle. *Anal. Sci.* **1990**, *6*, 67-70.